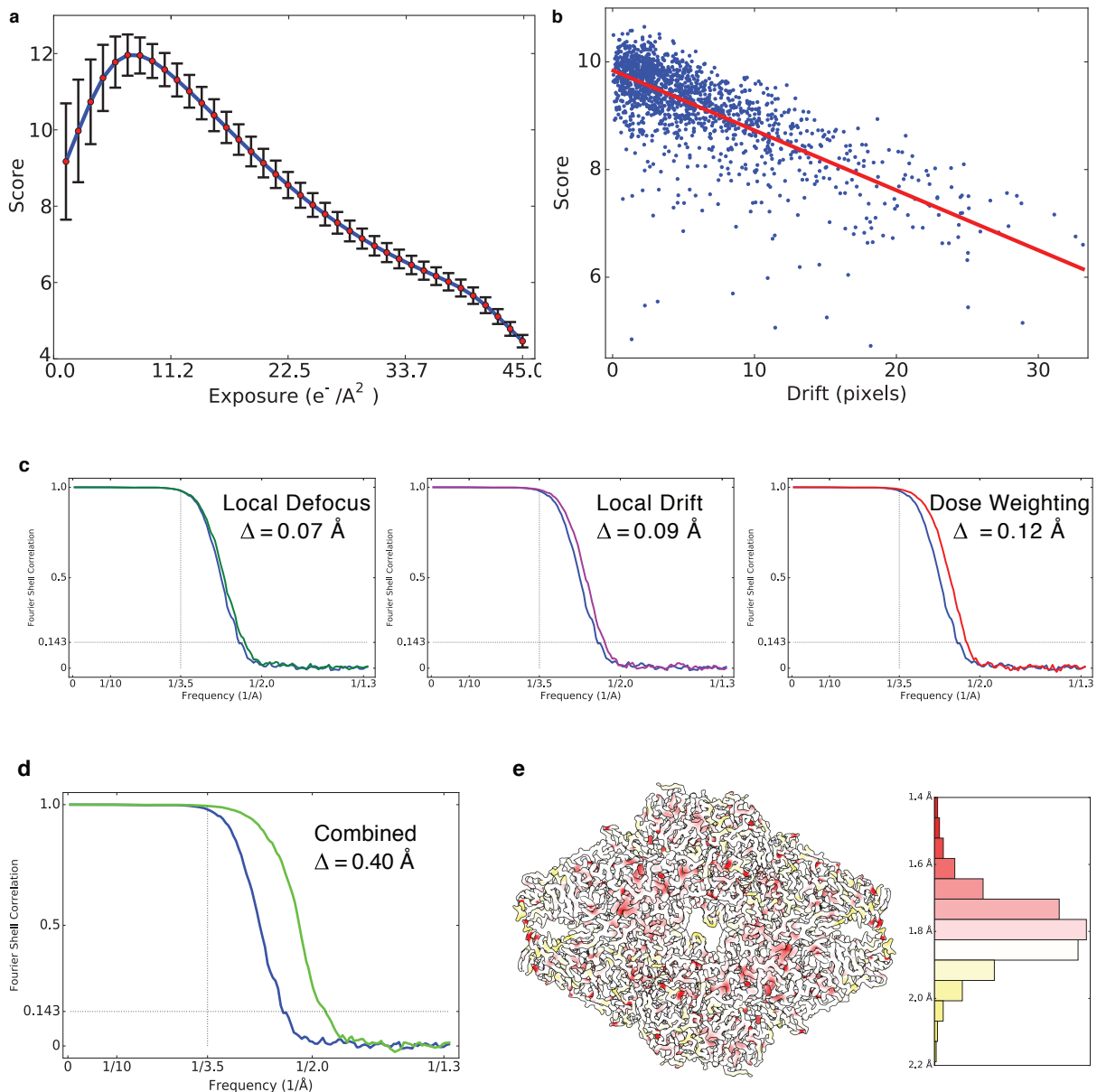


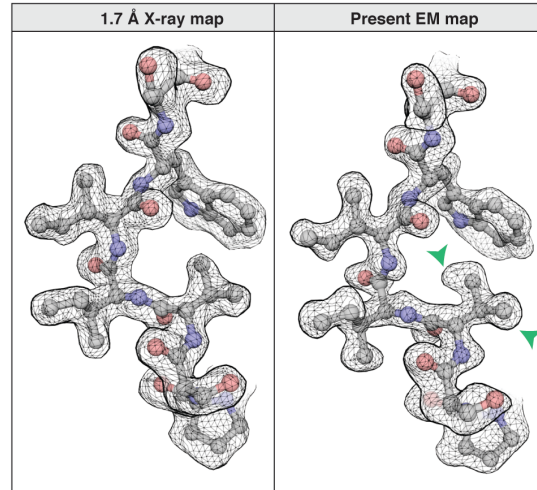
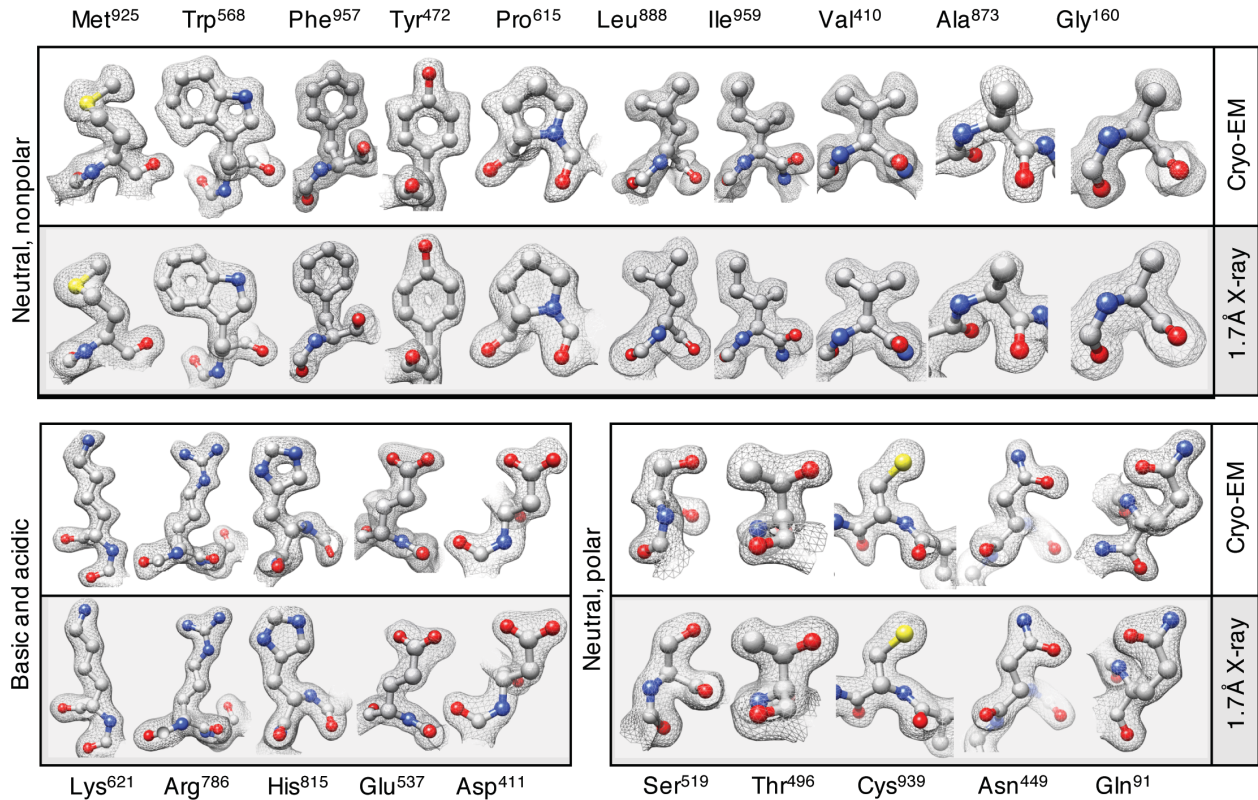
SUPPLEMENTARY FIGURES



Supplementary Figure 1. Data-driven dose weighting strategy based on per-particle FREALIGN score measurements and improvement in map resolution according to Fourier Shell Correlation (FSC) and local resolution metrics. Related to Figures 1 and 2.

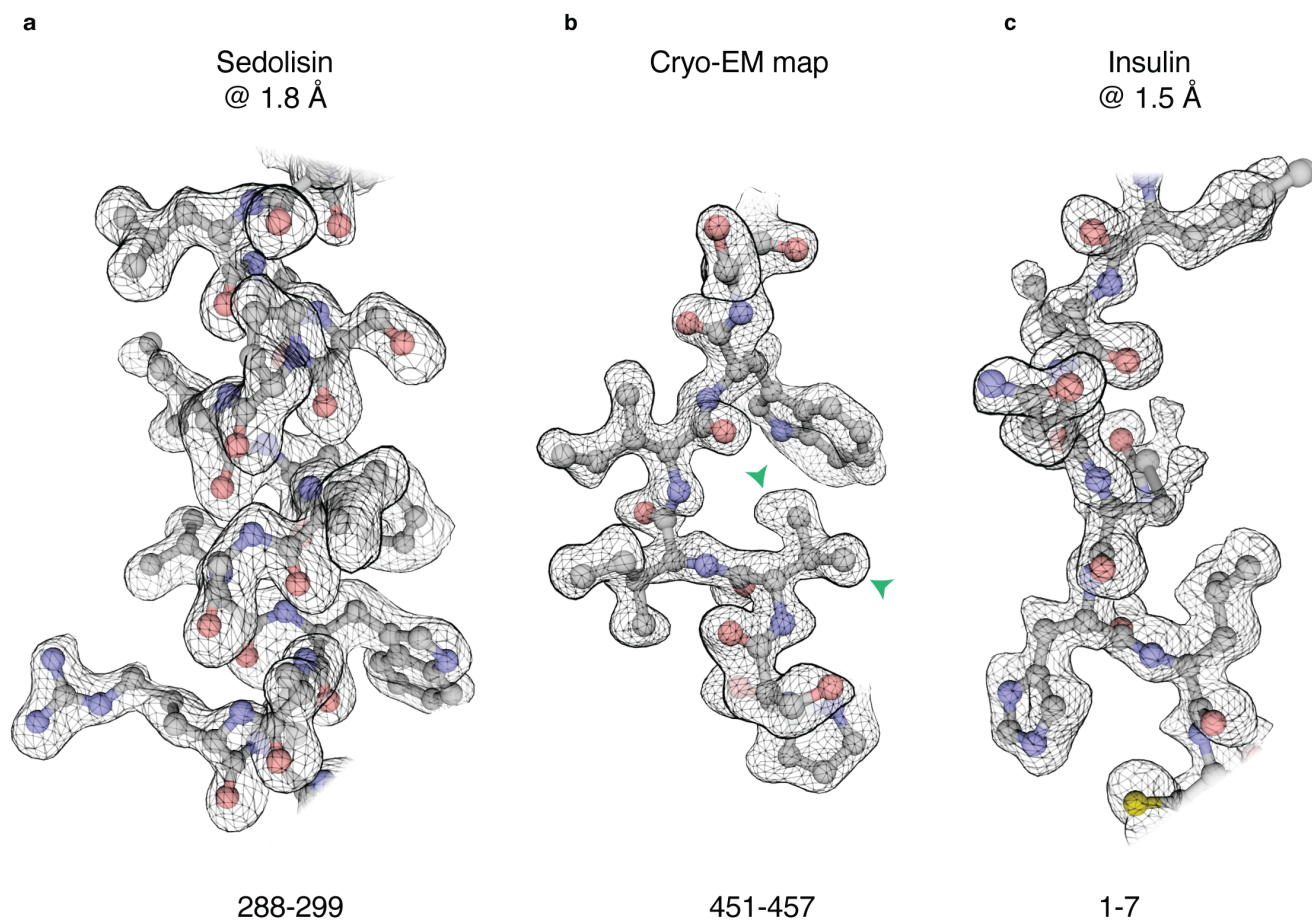
a) Average score values across all particles in dataset plotted as a function of the cumulative electron exposure. Vertical bars indicate the variance across all measurements, showing larger values at the beginning of the exposure and smaller values towards higher accumulated doses. **b)** Scatter plot of average score values assigned to the first frame of each movie versus amount of initial drift (scores were averaged across all particles in each movie and initial drift was measured between the first two frames of each movie using super-resolution pixel units). Red line indicates a linear fit to the data showing an inverse correlation between the amount of drift and the average score value. **c)** Resolution improvement

from each of the processing components of our strategy with respect to the 2.3 Å baseline reconstruction obtained using global frame alignment, global CTF estimation and the full exposure (blue curves). FSC curves between half-maps for reconstructions obtained using only local defocus correction (left, green curve), only local drift correction (middle, magenta curve), and only data-driven dose weighting (right, red curve), corresponding to resolution improvements of 0.07 Å, 0.09 Å, and 0.12 Å, respectively. **d)** Half-map FSC curve for the final reconstruction obtained by combining all three components of our approach, showing an overall resolution improvement of 0.4 Å (green curve, ~1.9 Å by 0.143 criterion) with respect to the 2.3 Å baseline reconstruction (blue curve). **e)** Color-coded cut-out surface representation of the β -galactosidase tetramer and corresponding 1D histogram showing local resolution values ranging from 2.2 Å to 1.4 Å in different regions of the protein measured by BLOCRES (Cardone et al., 2013).

a**b**

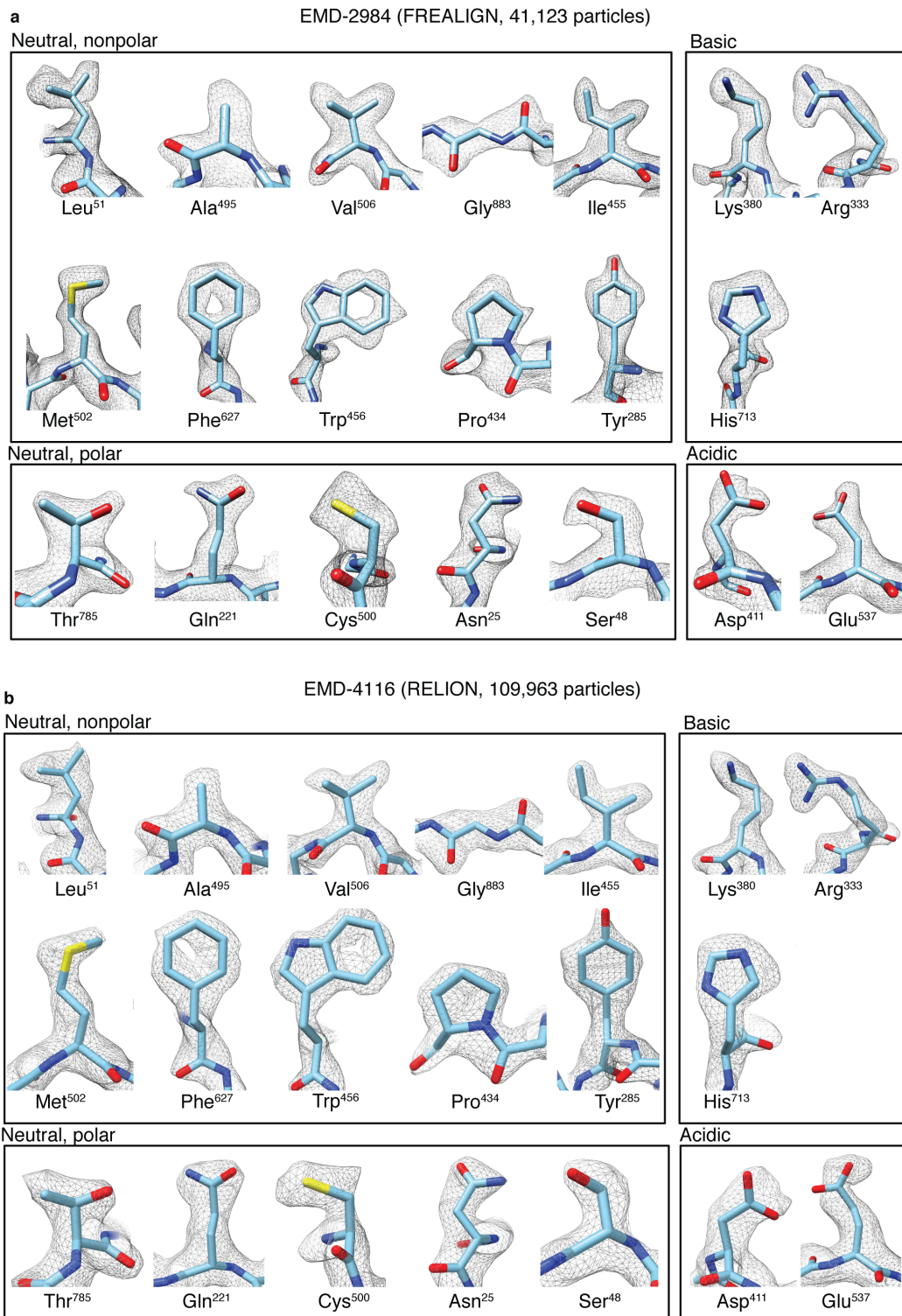
Supplementary Figure 2. Comparison of cryo-EM density map with 1.7 Å X-ray structure. [Related to Figure 2.](#)

a) Side-by-side comparison of region spanning residues 531- 541 between the 2Fo-Fc map computed from the 1.7 Å resolution X-ray structure (PDB ID 1DP0) and the new map. Green arrowheads highlight examples where the new cryo-EM map shows well-resolved outlines for individual atoms. **b)** Side-by-side comparison of density for each of the 20 amino acids between the X-ray and the cryo-EM maps.



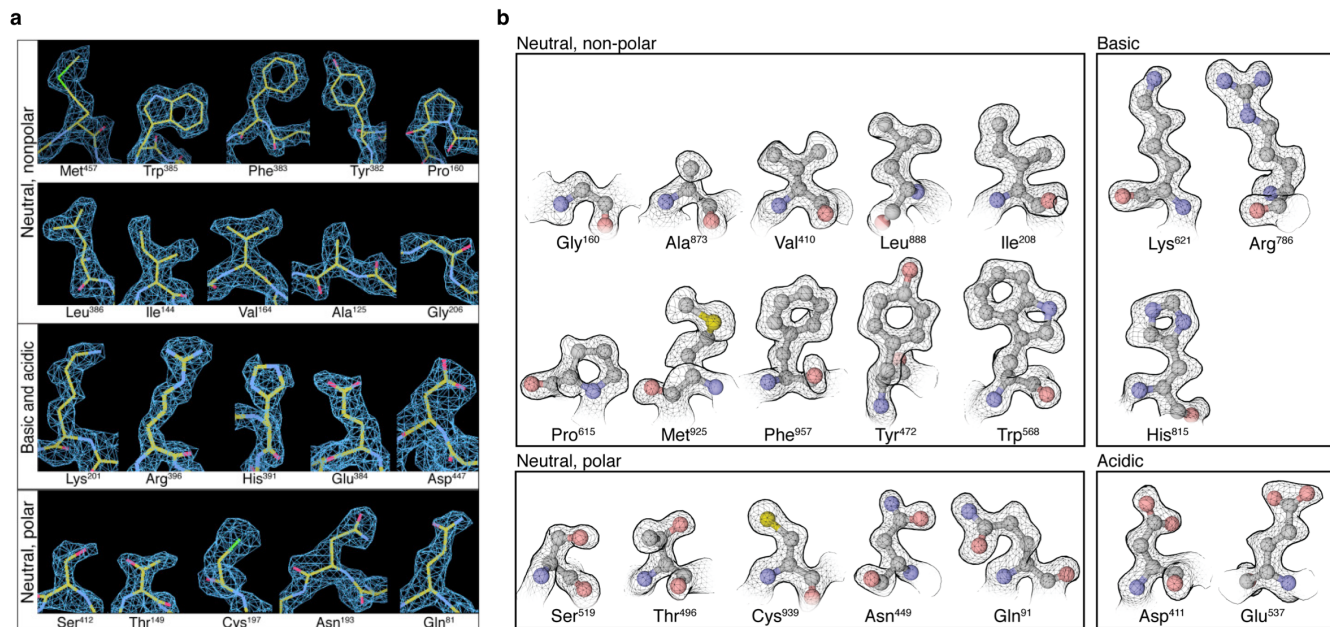
Supplementary Figure 3. Comparison of cryo-EM density map with 1.8 Å and 1.5 Å resolution X-ray maps obtained by anomalous scattering. Related to Figure 2.

Comparison of representative density features observed in the X-ray map of sedolisin at 1.8 Å resolution (residues 288-299, left), our cryo-EM map (residues 451-457, center) and the X-ray map of insulin at 1.5 Å resolution (residues 1-7, right). A qualitative evaluation of the delineation of punctate densities for non-H atoms suggest that the features observed in the most well-ordered regions of the cryo-EM density map are better resolved than in the 1.8 Å map of sedolisin and compare favorably with those seen in the 1.5 Å electron density map of insulin.



Supplementary Figure 4. Comparison of features between our previous 2.2 Å map and the RELION map. Related to Figure 3.

a-b) Side-by-side comparison of 20 amino acid panels as presented in Figure 4 of (Bartesaghi et al., 2015) between the previously published 2.2 Å map EMD-2984 obtained from ~40,000 particles (**a**), and map EMD-4116 obtained by Scheres and co-workers using RELION from ~110,000 particles (**b**).



Supplementary Figure 5. Comparison between the previously reported 1.8 Å map of glutamate dehydrogenase (GDH) and the present map. Related to Figure 2.

a-b) Side-by-side comparison of 20 amino acid panels from the 1.8 Å resolution map of GDH (reproduced from Figure 4 (Merk et al., 2016)) (a), and the present map of β -galactosidase (reproduced from Figure 2c) (b).